

# Investigation of Lithium Iodide Intercalated 2D- nanosheets for DSSC Applications

J. Babu\*, A. Antony Raj\*\*, J. Asghar\*, B. Arjun Kumar\*\*\*, Saravanan Sigamani\*\*\*\*, G. Ramalingam\*\*\*

\* Department of Physics, Islamiah College (A), Vaniyambadi (TN), India

\*\* Department of Physics, St. Joseph's College (A), Trichirapalli (TN), India

\*\*\* Quantum Materials Research Lab (QMRL), Department of Nanoscience & Technology, Alagappa University, Karaikudi (TN), India

\*\*\*\* Department of Nanotechnology, Swarnandhra College of Engineering & Technology (A), Narsapur, West Godavari (AP), India

‡

Corresponding Author; [j.asghar69@gmail.com](mailto:j.asghar69@gmail.com), [ramanloyola@gmail.com](mailto:ramanloyola@gmail.com)

Received: 22.07.2022 Accepted: 14.08.2022

**Abstract-** In the realm of solar energy conversion, dye sensitized solar cells (DSSCs) are gaining prominence. Typically, a counter electrode modification is required to improvement of DSSC efficiency; counter electrode materials that are  $WS_2$  and  $MoS_2$  in place of alternative for platinum (Pt). Pt is well recognized for its high cost and scarcity. In this study, a low-cost Pt-Free counter electrode was employed and determined solar cell efficiency of 2.52% over a long length of time. Further research on few layer  $WS_2$  and  $MoS_2$  nanosheets reveals increased solar efficiency. The acquired  $WS_2$  and  $MoS_2$  nanosheets has a shape that has been validated using a transmission electron microscope. Furthermore, the structural, optical, and functional groups of materials were described, and the probable mechanisms were examined.

**Keywords** Solar energy; DSSC; cell efficiency; nanoparticles; functional groups.

## 1. Introduction

At present, two-dimensional (2D) nanomaterials have been garnered great attention by owing to their unique properties at nanoscale level [1-3]. Among various materials, molybdenum disulfide ( $MoS_2$ ) and tungsten disulfide ( $WS_2$ ) is one among the 2D family and in particular it is described as a transition metal dichalcogenide (TMD) [4,5].  $MoS_2$  and  $WS_2$  have attracted the researchers become of their unique and tunable properties it structures alignment. It consist of one transition metal atom (Mo, W) connected by two sulfur atoms and stacked with the assistance of weak van der Waals forces[6,10]. By reducing the stacked layers of TMD, it provides enhanced and improved physical,

chemical and optical properties. This few layered  $MoS_2$  and  $WS_2$  nanosheets are employed in various applications like photo catalysis, flexible electronics, super capacitors, Li-ion batteries, dye sensitized solar cells [9–10]. To reduce the stacked layers in  $MoS_2$  and  $WS_2$  numerous methods have been handled by the researchers such as hydrothermal, mechanical exfoliation and liquid phase exfoliation [11–15]. The above synthesis techniques had some drawbacks like long time synthesis, high-cost solvents and uneven exfoliation. To overcome this flaws lithium intercalation method was introduced to synthesis the effective way to exfoliate and stabilize the few layer nanosheets. Lithium intercalation method is the predominant method for exfoliation of layers and rapid synthesis of  $MoS_2$  and  $WS_2$

nanosheets. Crystalline MoS<sub>2</sub> and WS<sub>2</sub> possess two phases such as 2-hexagonal symmetry and 3-rhombohedral symmetry. At every layer the two phases have similar atomic coordination [16,17]. Dye sensitized solar cells (DSSC) is one of the most promising technologies in energy harvesting owing to low-cost manufacturing, large scale fabrication and their stability. DSSC have possessed different layers to generate electrons and their components are photo anode, dye solution, electrolyte and counter electrodes. Counter electrode is the main part in DSSC and it receives the electron from the anode and transfers to the electrolyte. Mostly platinum (Pt) was used as counter electrode due its high electro catalytic activity. To replace Pt because of its high cost, TMD's were introduced as a counter electrode [18,19].

In the current work, we synthesized simple and effective method of microwave assisted lithium intercalation of MoS<sub>2</sub> and WS<sub>2</sub> is described. The as prepared MoS<sub>2</sub> and WS<sub>2</sub> few layer nanosheets were studied physical, chemical and optical properties and the nanosheets were introduced as counter electrode of the dye sensitized solar cells.

## 2. Materials and Methods

### 2.1 Materials

All the chemicals were analytical grade and used without additional purification. Initially, the primary sources of the materials are purchased from Alfa Aesar such as molybdenum (IV) sulfide (98%), and tungsten sulfide (98%). The FTO glass substrate, polyethylene oxide (PEO), polyethylene glycol (PEG), N719 ruthenium dye, polyvinylidene fluoride, N-Methyl-2-Pyrrolidone, Lithium iodide (Li-I), 1-propyl-2,3-dimethylimidazolium iodide, acetonitrile were procured from the Sigma-Aldrich company. Furthermore, the double distilled water (H<sub>2</sub>O) used throughout the experiment.

### 2.2 Methods

The XS<sub>2</sub> (X = Mo, W) nanosheets were synthesized through a microwave irradiation method using lithium hydroxide. In brief, 0.1g of XS<sub>2</sub> powder and 0.057g of LiOH.2H<sub>2</sub>O were dispersed in 30ml of ethylene glycol (EG). Next, this mixture continuously stirred for 1 hour until it becomes a homogeneous mixture at a temperature about 70°C. Then the homogeneous mixture was heated in a microwave oven and the process was repeated 12 times at 50 watts by interval of 1 mi-

nute. The heated solution was naturally cooled down at room temperature. The above solution was kept under the bath sonication for 30 minutes, at the room temperature. The mixture was centrifuged for 25 minutes at 2000 rpm for 5 times. Finally, the obtained precipitate collected and washed by using acetone at several times to eliminate the excess solution of EG. Then the precipitate was dried by 100°C using hot-air oven for 6 hrs. Figure 1 shows the schematic representation of MoS<sub>2</sub>, WS<sub>2</sub> preparation.

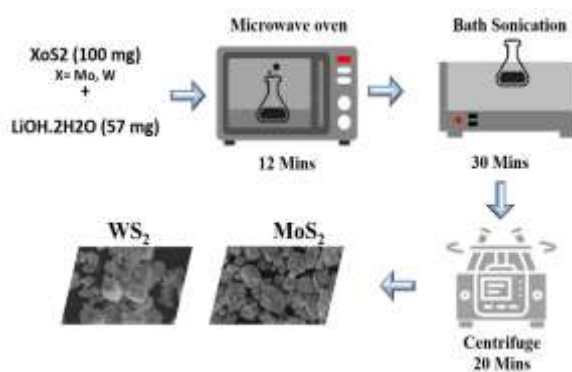


**Fig. 1.** Schematic representation of synthesis of MoS<sub>2</sub>, WS<sub>2</sub> nanosheets.

### 2.3 Fabrication of DSSC

The DSSC device fabrication process is discussed (Figure 2) in detail below. First, FTO substrates were cleaned using soap, detergent solution, double distilled water, and acetone in bath sonicator and then dried at 70°C for 30 min. The TiO<sub>2</sub> nanoparticles combined with PEO, PEG, and other organic solvents were used for the preparation of photo anodes. The final paste was coated on cleaned FTO substrates using Doctor Blade method and annealed at the 500°C for 30 min. This photoanode soaked into the N719 ruthenium dye (3mM) for 24 hrs and then the substrates were washed by several times using ethanol.

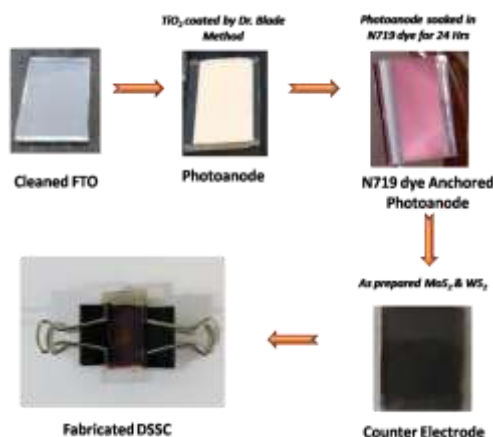


**Fig.2.** Photograph of device fabrication of DSSC.

The counter electrode from MoS<sub>2</sub> and WS<sub>2</sub> (95mg) and polyvinylidene fluoride (5 mg) blended with N-Methyl-2-Pyrrolidone (NMP) and the resulted slurry was deposited on cleaned-FTO substrate and dried at 70°C for 12 hrs. Next, Iodide/Triiodide used as an electrolyte were injected into the active area, followed by dye anchored photoanode and counter electrode were sandwiched to fabricate the complete DSSC device [8]. Figure 2 shows the step-by-step preparation of solace device on FTO substrate.

### 3. Results and Discussion

#### 3.1. XRD

The XRD patterns of WS<sub>2</sub> and MoS<sub>2</sub> are shows in figure 3. The XRD pattern indicates the WS<sub>2</sub> and MoS<sub>2</sub> phase structure with high purity of both samples. The intense diffraction peaks of WS<sub>2</sub> are noticed at 14.3°, 28.67°, 32.7°, 39.34°, 43.63°, 49.65°, 59.11°, 60° and 62.1° corresponding to the reflection planes of (002), (004), (100), (103), (006), (110), (112), and (107). Next, MoS<sub>2</sub> are observed peaks were appeared in 14.3°, 29.02°, 44.16°, 60.11° associate with (002), (004), (006), (008). This diffraction peaks are confirmed and evidenced with the standard JCPDS file # 08-0237 and 37-1492. These peaks indicate the stacking of few-layered sheets along the C-axis and the presence of the hexagonal phase was reduced when lithium intercalation and microwave irradiation process [20,21]. Applying the XRD Pattern crystallite size were find using Scherrer formula  $D_p = K\lambda/\beta \cos\theta$  here, K is shape factor,  $\lambda$  wavelength of X-ray (1.54178 Å),  $\beta$  = FWHM of XRD peak,  $\theta$  = peak position and  $D_p$  = crystallite size. Calculated crystallite size of WS<sub>2</sub> and MoS<sub>2</sub> is 26.58 nm and 32.74 nm, respectively. The crystallite size defines the size of the sheets the variation of sizes influences in the applications.

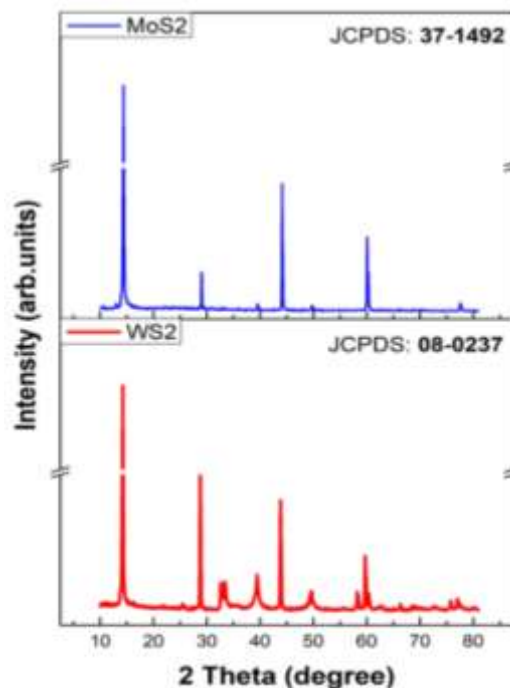


**Fig.3.** X-ray diffraction pattern of MoS<sub>2</sub> and WS<sub>2</sub> nanosheets.

#### 3.2. Raman Spectrum

Raman spectroscopy measurements performed to further confirm the phase classification as shown in figure 4. This characteristic Raman shifts occurred at 325, 450 cm<sup>-1</sup> 366 and 431 cm<sup>-1</sup> corresponding to WS<sub>2</sub> and MoS<sub>2</sub>. It is clearly expected for the E<sub>12g</sub> and A<sub>1g</sub>, respectively. Further, the additional (weak) peaks at lower frequency regions are corresponding to modes such as active 1T-type WS<sub>2</sub> and MoS<sub>2</sub>. It's not allowed in 2H-WS<sub>2</sub>. Besides, the Raman spectra were monitored as a function of the calcination temperatures. These spectra were revealed that the intensities of the Raman active modes don't change after the exfoliation process. In addition, the positions of E<sub>12g</sub> and A<sub>1g</sub> peaks were reported to change with the number of monologues and weak down shift also observed for bulk WS<sub>2</sub> and MoS<sub>2</sub> [22,23].

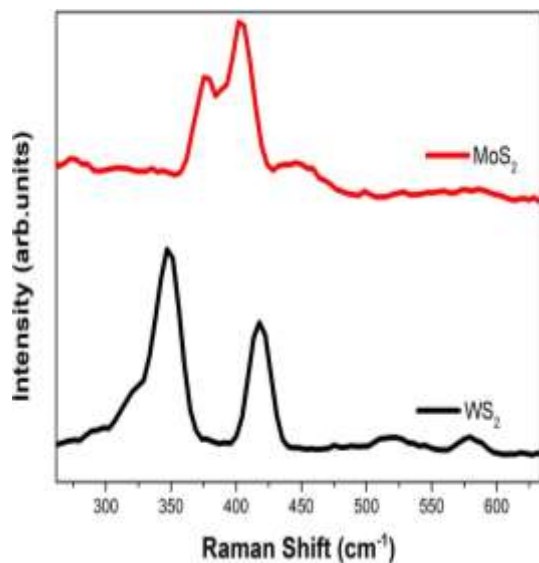


**Fig. 4.** Raman pattern of MoS<sub>2</sub> and WS<sub>2</sub> nanosheets.

### 3.3. UV-Visible Absorbance

Figure 5 shows the UV-Visible spectrum that clearly shows the absorbance spectrum of MoS<sub>2</sub> and WS<sub>2</sub>. The direct excitonic transition expected from the deep valence band (VB) to the conduction band (CB) and evidenced results by the absorption bands at 459, 616 and 669 nm could be endorsed to the existence transitions from the 'K' point of the Brillouin zone. All of these characteristic peaks demonstrated better agreement with few-layered 2H-MoS<sub>2</sub>. Another, WS<sub>2</sub> nanosheets peaks were presented in 640 and 520 nm.

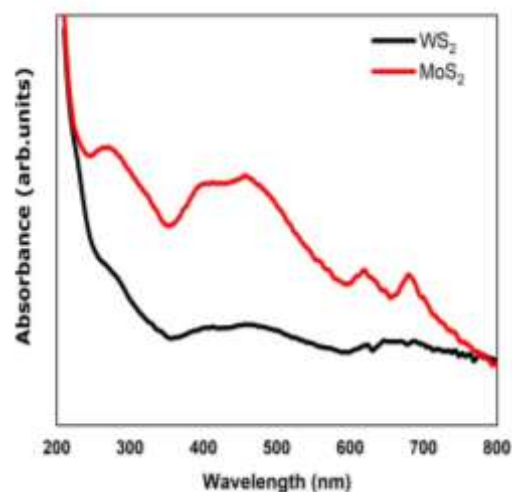


**Fig. 5.** UV-Visible Spectrum of few layer MoS<sub>2</sub> and WS<sub>2</sub> nanosheets.

### 3.4. Scanning Electron Microscopy (SEM)

Synthesized WS<sub>2</sub> and MoS<sub>2</sub> were treated for an SEM observation to study about the morphology of the microwave assisted Li-intercalated few layers of MoS<sub>2</sub> and WS<sub>2</sub> which were shown in Fig. 6 (a-e). It shows the morphological image of MoS<sub>2</sub> in different magnification. Thereby it shows the distinct nano sheets appeared in the image. This shows the exfoliation process was done in both the directions like reducing of layer thickness and size of sheets. The SEM image of WS<sub>2</sub>, MoS<sub>2</sub> Fig. 6(a-d) depicted the randomly arranged hexagonal shape of exfoliated WS<sub>2</sub> and MoS<sub>2</sub> catalysts, which are arranged in a symmetrical manner. Moreover, the reduced plate width and multi-layer formations are noticed.

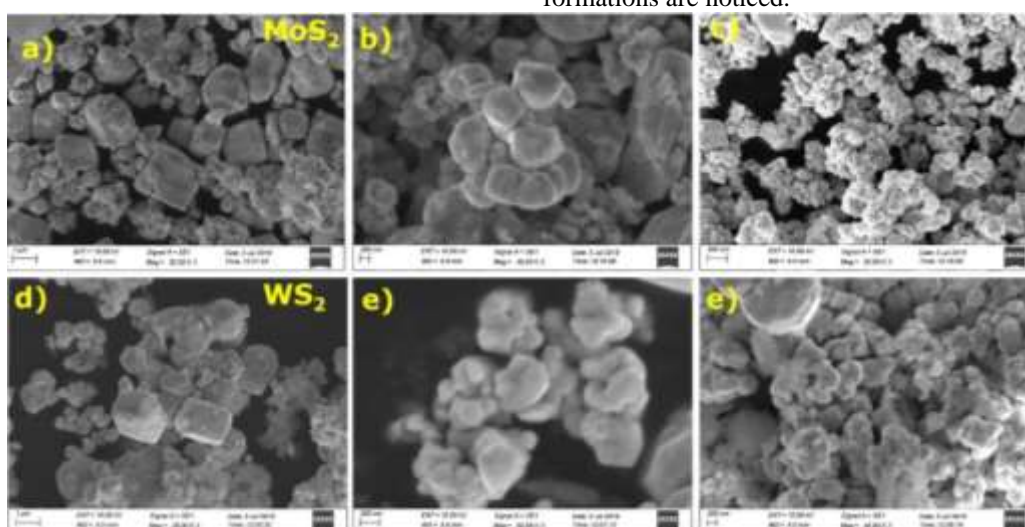


**Fig. 6.** SEM images of as synthesized few layers MoS<sub>2</sub> and WS<sub>2</sub> nanosheets.

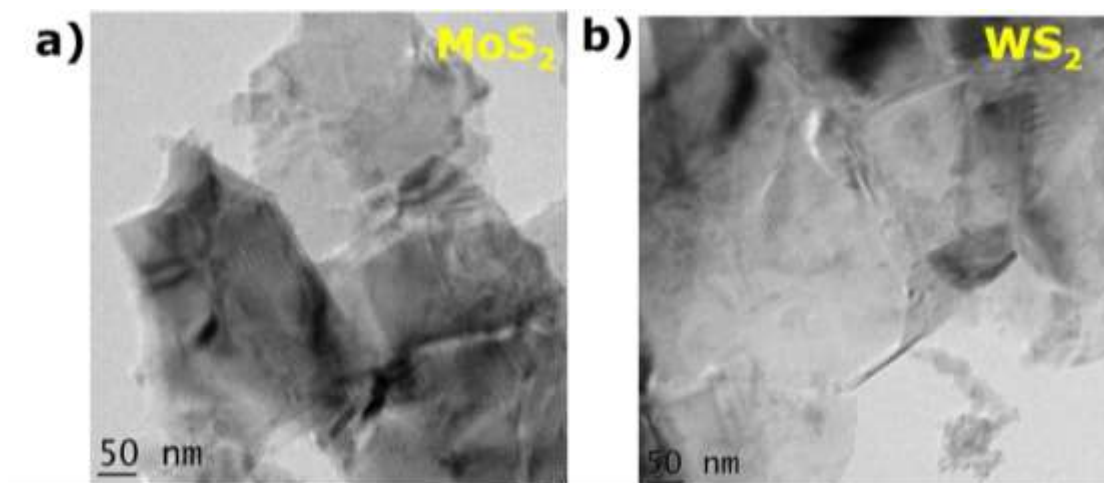


**Fig. 7.** TEM images of MoS<sub>2</sub>(a) WS<sub>2</sub>(b) nanosheets.

The corresponding peak to the (002) plane presented in the XRD pattern (Figure 1) which supports to the Figure 6 (b, e), where WS<sub>2</sub> and MoS<sub>2</sub> platelets stacked together with highly ordered packing. Further, Transmission electron microscope (TEM) was employed to observe the morphological structure of the XS<sub>2</sub>. Figure 7 shows the TEM images of MoS<sub>2</sub> and WS<sub>2</sub> which shows the clear transparent sheets of MoS<sub>2</sub>, WS<sub>2</sub> and it confirms that the bulk MoS<sub>2</sub>, WS<sub>2</sub> has been well exfoliated and retains a few layers of 2D- sheets.

### 3.5. DSSC Performance

The prepared MoS<sub>2</sub>, WS<sub>2</sub> Samples were introduced to the counterpart of dye sensitized solar cells (DSSC). Figure 8 shows the light trapping scheme and possible mechanism of MoS<sub>2</sub>, WS<sub>2</sub> solar cell device assembly. The fabricated DSSC devices of MoS<sub>2</sub> and WS<sub>2</sub> are delivered the photo-conversion efficiency ( $\eta$ ) of 2.15% and 2.52%, respectively.

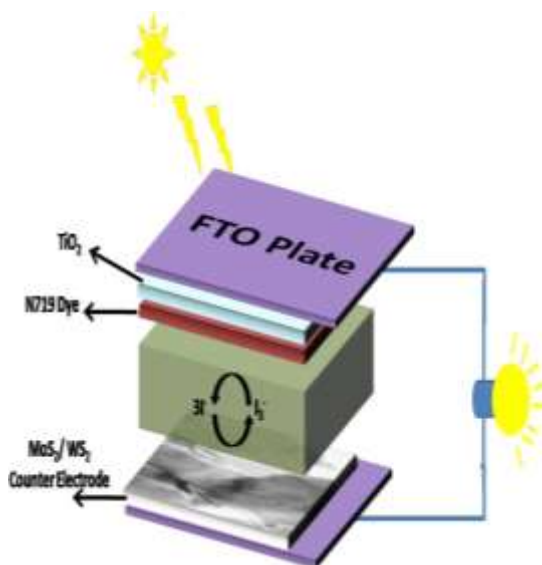


**Fig. 8.** Scheme and possible mechanism of XS<sub>2</sub> solar cell device assembly.

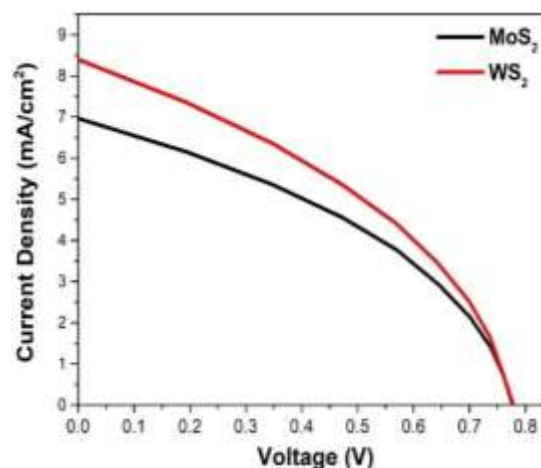


**Fig. 9.** J-V curve of fabricated DSSC using MoS<sub>2</sub> and WS<sub>2</sub>.

**Table 1.** Dye sensitized solar cell parameters for as synthesized MoS<sub>2</sub> and WS<sub>2</sub>

Sample	Voc (V)	Jsc (mA/cm <sup>2</sup> )	FF	η (%)
MoS <sub>2</sub>	0.78	6.96	0.39	2.15
WS <sub>2</sub>	0.78	8.42	0.38	2.52

Solar cell parameter of MoS<sub>2</sub> had an open circuit voltage (V<sub>OC</sub>), short circuit current density (J<sub>sc</sub>) and its fill factor (FF) are tabulated (Table-I) and J-V curve has been shown in Figure 9. MoS<sub>2</sub> provides V<sub>oc</sub> of 0.78 V, J<sub>sc</sub> of 6.96 mA/cm<sup>2</sup>, fill factor of 0.39% and WS<sub>2</sub> gives 0.78 V(V<sub>oc</sub>), 8.42 mA/cm<sup>2</sup> (J<sub>sc</sub>), 0.38 % (FF). The results clearly delivered that performance of DSSC was improved because of the presence of few layered nanosheets of MoS<sub>2</sub> and WS<sub>2</sub> this may confirm through XRD and TEM the lower sized crystallite size sample provided high efficiency. The few layered nanosheets have possessed good electrocatalytic activity, high surface area, stability towards the corrosion caused by electrolyte [24].

#### 4. Conclusion

In summary, we have successfully prepared the lithium iodide intercalated MoS<sub>2</sub>, the WS<sub>2</sub> 2D-nanosheets using the simple and rapid process microwave assisted method. The microwave technique helps to intercalation and loosen of the bulk sheets, loosen sheets were exfoliated with the help of sonication process the resultant shows few layers of 2D nanosheets. Compared to MoS<sub>2</sub>, the WS<sub>2</sub> nanolayer has shown increased dye sensitized solar cell efficiency (2.15 and 2.52 %) because of highest Lithium-ion intercalation on WS<sub>2</sub> layer. The TEM images of MoS<sub>2</sub> and WS<sub>2</sub> shows clear transparent sheets. In future, the parameter optimization could be useful for the enhancement of better photovoltaic performance.

#### Acknowledgements

The corresponding author Dr. G. Ramalingam acknowledges the financial support from MHRD-SPARC-890 (2019) DST-SERB 198/2016. The instrumentation facility utilized from RUSA2.0 grant No.F.24-51/2014-U, Policy (TN MultiGen) Govt. of India Projects.

#### References

- [1] F. Ghasemzadeh, M. Esmailzadeh, and M.E. Shayan, "Photovoltaic temperature challenges and bismuthene monolayer properties", *International Journal of Smart Grid*, vol. 4, pp. 190-195, December 2020. <https://doi.org/10.20508/ijsmartgrid.v4i4.131.g109>
- [2] K.E. Okedu, A. Al Senaidi, I. Al Hajri, I. Al Rashdi, and W. Al Salmani, "Real time dynamic analysis of solar PV integration for energy optimization", *International Journal of Smart Grid*, vol. 4, pp. 68-79, June 2020.
- [3] Kenneth E. Okedu, and M.Al-Hashmi, "Assessment of the cost of various renewable energy systems to provide power for a small community: case of Bukha, Oman", *International Journal of Smart Grid*, vol. 3, pp. 172-182, August 2018. <https://doi.org/10.20508/ijsmartgrid.v2i3.17.g179>
- [4] S. Manzeli, D. Ovchinnikov, D. Pasquier, O.V. Yazyev, and A. Kis, "2D transition metal dichalcogenides", *Nat. Rev. Mater.*, vol. 2, pp. 17033, June 2017. <https://doi.org/10.1038/natrevmats.2017.33>
- [5] A. Jawaaid, D. Nepal, K. Park, M. Jespersen, A. Qualley, P. Mirau, L.F. Drummy, and R.A. Vaia, "Mechanism for liquid phase exfoliation of MoS<sub>2</sub>", *Chem. Mater.*, vol. 28, pp. 337-348, December 2016. <https://doi.org/10.1021/acs.chemmater.5b04224>.
- [6] X. Cai, Y. Luo, B. Liu, and H.-M. Cheng, "Preparation of 2D material dispersions and their applications", *Chem. Soc. Rev.*, vol. 47, pp. 6224-6266, June 2018. <https://doi.org/10.1039/C8CS00254A>.
- [7] Q. Cao, F. Grote, M. Hubmann, and S. Eigler, "Emerging field of few-layered intercalated 2D materials", *Nanoscale Adv.*, vol. 3, pp. 963-982, January 2021. <https://doi.org/10.1039/D0NA00987C>.
- [8] K. Dharamalingam, B. Arjun Kumar, G.

- Ramalingam, S. Sasi Florence, K. Raju, P. Senthil Kumar, S. Govindaraju, and E. Thangavel, "The role of sodium dodecyl sulfate mediated hydrothermal synthesis of MoS<sub>2</sub> nanosheets for photocatalytic dye degradation and dye-sensitized solar cell application", *Chemosphere*, vol. 294, pp. 133725, May 2022. <https://doi.org/10.1016/j.chemosphere.2022.133725>.
- [9] B.A. Kumar, V. Vetrivelan, G. Ramalingam, A. Manikandan, S. Viswanathan, P. Boomi, and G. Ravi, "Computational studies and experimental fabrication of DSSC device assembly on 2D-layered TiO<sub>2</sub> and MoS<sub>2</sub>@TiO<sub>2</sub> nanomaterials", *Phys. B Condens. Matter*, vol. 633, pp. 413770, May 2022. <https://doi.org/10.1016/j.physb.2022.413770>
- [10] Y. Li, K. Chang, Z. Sun, E. Shangguan, H. Tang, B. Li, J. Sun, and Z. Chang, "Selective preparation of 1T- and 2H-phase MoS<sub>2</sub> nanosheets with abundant monolayer structure and their applications in energy storage devices", *ACS Appl. Energy Mater*, vol. 3, pp. 998–1009, January 2020. <https://doi.org/10.1021/acsaem.9b02043>.
- [11] M. Yi, Z. Shen, S. Ma, and X. Zhang, "A mixed-solvent strategy for facile and green preparation of graphene by liquid-phase exfoliation of graphite", *J. Nanoparticle Res*, vol. 14, July 2012. <https://doi.org/10.1007/s11051-012-1003-5>.
- [12] M. Gurulakshmi, A. Meenakshamma, G. Siddeswaramma, K. Susmitha, Y.P. Venkata Subbaiah, T. Narayana, and M. Raghvender, "Electrodeposited MoS<sub>2</sub> counter electrode for flexible dye sensitized solar cell module with ionic liquid assisted photoelectrode", *Sol. Energy*, vol. 199, pp. 447-452, March 2020. <https://doi.org/10.1016/j.solener.2020.02.047>
- [13] H. Zhao, H. Wu, J. Wu, J. Li, Y. Wang, Y. Zhang, and H. Liu, "Preparation of MoS<sub>2</sub>/WS<sub>2</sub> nanosheets by liquid phase exfoliation with assistance of epigallocatechin gallate and study as an additive for high-performance lithium-sulfur batteries", *J. Colloid Interface Sci*, vol. 552, pp. 554–562, September 2019. <https://doi.org/10.1016/j.jcis.2019.05.080>.
- [14] S. Luo, S. Dong, C. Lu, C. Yu, Y. Ou, L. Luo, J. Sun, and J. Sun, "Rational and green synthesis of novel two-dimensional WS<sub>2</sub>/MoS<sub>2</sub> heterojunction via direct exfoliation in ethanol-water targeting advanced visible-light-responsive photocatalytic performance", *J. Colloid Interface Sci*, vol. 513, pp. 389–399, March 2018. <https://doi.org/10.1016/j.jcis.2017.11.044>.
- [15] C. Backes, N.C. Berner, X. Chen, P. Lafargue, P. LaPlace, M. Freeley, G.S. Duesberg, J.N. Coleman, and A.R. McDonald, "Functionalization of liquid-exfoliated two-dimensional 2H-MoS<sub>2</sub>", *Angew. Chemie*, vol. 127, pp. 2676–2680, January 2015. <https://doi.org/10.1002/ange.201409412>.
- [16] M. Rajapakse, B. Karki, U.O. Abu, S. Pishgar, M.R.K. Musa, S.M.S. Riyadh, M. Yu, G. Sumanasekera, and J.B. Jasinski, "Intercalation as a versatile tool for fabrication, property tuning, and phase transitions in 2D materials", *Npj 2D Mater. Appl*, vol. 5, pp. 30, March 2021. <https://doi.org/10.1038/s41699-021-00211-6>.
- [17] F. Xiong, H. Wang, X. Liu, J. Sun, M. Brongersma, E. Pop, and Y. Cui, "Li intercalation in MoS<sub>2</sub>: in situ observation of its dynamics and tuning optical and electrical properties", *Nano Lett*, vol. 15, pp. 6777–6784, September 2015. <https://doi.org/10.1021/acs.nanolett.5b02619>.
- [18] M. Caruso, R. Miceli, P. Romano, G. Schettino, and F. Viola, "Technical and economical performances of photovoltaic generation facades", *International Journal of Smart Grid*, vol. 2, pp. 87-98, June 2018. DOI:10.20508/ijsmartgrid.v2i2.19.g19
- [19] B. Arjun Kumar, P. Kumar, T. Elangovan, G. Ramalingam, G. Ravi, P. Mohanapriya, and T.S. Natarajan, "Surface functionalization of core-shell QDs for solar photovoltaic and anti-cancer applications", *Appl. Surf. Sci. Adv*, vol. 5, pp.100122, September 2021. <https://doi.org/10.1016/j.apsadv.2021.100122>.
- [20] W. Liu, C. Zhao, R. Zhou, D. Zhou, Z. Liu, and X. Lu, "Lignin-assisted

- exfoliation of molybdenum disulfide in aqueous media and its application in lithium ion batteries", *Nanoscale*, vol. 7, pp. 9919–9926, April 2015. <https://doi.org/10.1039/C5NR01891A>.
- [21] E.P. Nguyen, B.J. Carey, T. Daeneke, J.Z. Ou, K. Latham, S. Zhuiykov, and K. Kalantar-Zadeh, "Investigation of two-solvent grinding-assisted liquid phase exfoliation of layered MoS<sub>2</sub>", *Chem. Mater.*, vol. 27, pp. 53–59, January 2015. <https://doi.org/10.1021/cm502915f>.
- [22] M.S. Gilliam, A. Yousaf, Y. Guo, D.O. Li, A.A. Momenah, Q.H. Wang, and A.A. Green, "Evaluating the exfoliation efficiency of quasi-2D metal diboride nanosheets using hansen solubility parameters", *Langmuir*, vol. 37, pp. 1194–1205, January 2021. <https://doi.org/10.1021/acs.langmuir.0c03138>.
- [23] D. Nakamura, and H. Nakano, "Liquid-phase exfoliation of germanane based on hansen solubility parameters", *Chem. Mater.*, vol. 30, pp. 5333–5338, July 2018. <https://doi.org/10.1021/acs.chemmater.8b02153>.
- [24] S. Kyaligonza, and E. Cetkin, "Photovoltaic system efficiency enhancement with thermal management: Phase changing materials (PCM) with high conductivity inserts", *International Journal of Smart Grid*, vol. 4, pp. 138-148, December 2021. <https://doi.org/10.20508/ijsmartgrid.v5i4.218.g171>.